Accurate Prediction of Band Gaps in Neutral Heterocyclic Conjugated Polymers

Geoffrey R. Hutchison, Mark A. Ratner,* and Tobin J. Marks*

Department of Chemistry and the Materials Research Center, Northwestern University, Evanston, Illinois 60208-3113

Received: April 23, 2002; In Final Form: August 8, 2002

Heterocyclic π-electron polymers such as polythiophene, polypyrrole, and polyfuran attract wide interest on both experimental and theoretical levels. While the optical properties of these materials are dominated by the band gap, no accurate, reliable computational method currently exists to predict the band gaps of large oligomers. Six computational methods, including ZINDO/CIS, ZINDO/RPA, HF/CIS, HF/RPA, TDDFT/TDA, and TDDFT are compared here for a set of 60 structurally well-defined heterocyclic oligomers of varied structure. All six methods are compared using both AM1 semiempirical and B3LYP DFT predicted geometries. Among the methods, the semiempirical ZINDO/CIS method applied to DFT-predicted geometries affords the best agreement between computed and experimental band gaps, yielding an RMS error of 0.31 eV over the data set considered. Analysis of the computed band gaps provides a simple, straightforward empirical correction that significantly improves the accuracy of all six methods, with RMS errors between 0.23 eV and 0.44 eV for TDDFT using DFT-predicted geometries and for ZINDO/RPA using AM1-predicted geometries, respectively.

I. Introduction

The field of electronically and photonically active conjugated polymers has generated intense scientific and technological interest since initial reports of dramatic increases in conductivity upon halogen doping of polyacetylene in the 1970s.[1−4] Second-generation polymers include polyheterocyclic macromolecules such as polythiophenes,[5,6] polypyrroles,[7] and polyfurans,[8−10] in addition to hydrocarbons such as poly(*p*-phenylenevinylene).[11] As well as the polymers themselves, discrete oligomers are widely studied as informative models for the polymers[12,13] and as useful materials in their own right.[12] Applications of such conjugated polymers are now wide-ranging, and include conducting fabrics,[14] thin-film field effect transistors,[15,16] organic light-emitting diodes (OLEDs),[17−19] and photovoltaic devices.[20,21]

Reliable and accurate methods for predicting the electronic structure of the aforementioned macromolecules would afford better understanding of structure−property relationships for tailoring physical characteristics such as optical transparency, color, electrical conductivity, majority carrier type (*n* or *p*), and electroluminescence. In OLED devices, there is a need for targeting emissive chromophores that span the spectrum of visible light[22−27] and especially a need for blue-emitters.[28] Organic photovoltaic devices also require light-harvesting structures that can span a wide range of photon input energies.[29,30] Furthermore, rationally designed transparent conducting polymers are needed to supplement or replace inorganic transparent conducting oxides in numerous applications. Importantly, addressing any of these challenges requires accurate and computationally efficient prediction of the optical band gap for tuning absorption[31] as well as the position of the plasma frequency for minimizing reflectivity.[2]

A fundamental challenge in organic electronic materials development is the establishment of reliable, instructive, and computationally efficient theoretical methodologies for predicting the optical properties of new substances. Such methodologies should ideally have high predictive accuracy over wide ranges of both molecular structures, compositions, and absorption energies. For example, torsional effects in some polymers and oligomers disrupt the conjugated π-system, so an accurate methodology should be capable of treating this partial overlap between neighboring monomer units. Additionally, the most common approximation for predicting band gaps of conjugated polymers relies on extrapolating the band gap of the full polymer from the scaling of the band gaps of a series of oligomeric molecules having increasing lengths.[13,32−34] While it is not clear that this approximation is particularly accurate, especially when compared to explicit calculations on the polymer itself,[35] to be useful such an approach requires that the computational methodology employed not only incur small errors overall, but also is well-matched to both large and small π-systems. Since some semiempirical models, such as ZINDO, were parametrized on small molecules,[36] and not on oligomers, they may not be appropriate for this extrapolation.

To compare how well current methods address this problem, we have compiled a set of experimental solution-phase λ_{max} optical absorption data for various conjugated, well-defined thiophene, pyrrole, and furan oligomers.[5,7,9,37−48] The set spans oligomer lengths from one to seven monomer units, and includes both molecules expected to be almost perfectly planar and some expected to have significant dihedral angles between neighboring rings. No data for polymers are included since molecular weight distribution data are seldom reported. Additionally, all molecules discussed in this work are uncharged, (i.e., undoped). While the doped materials are more electrically conductive than undoped counterparts, few experimental optical measurements on cationic or anionic oligomers have been reported for comparison.[49] Additionally, treating closed-shell molecules simplifies the computational methods needed for the comparisons.

* Corresponding authors. E-mail: ratner@chem.northwestern.edu, t-marks@northwestern.edu.

10.1021/jp025999m CCC: $22.00
Published on Web 10/08/2002

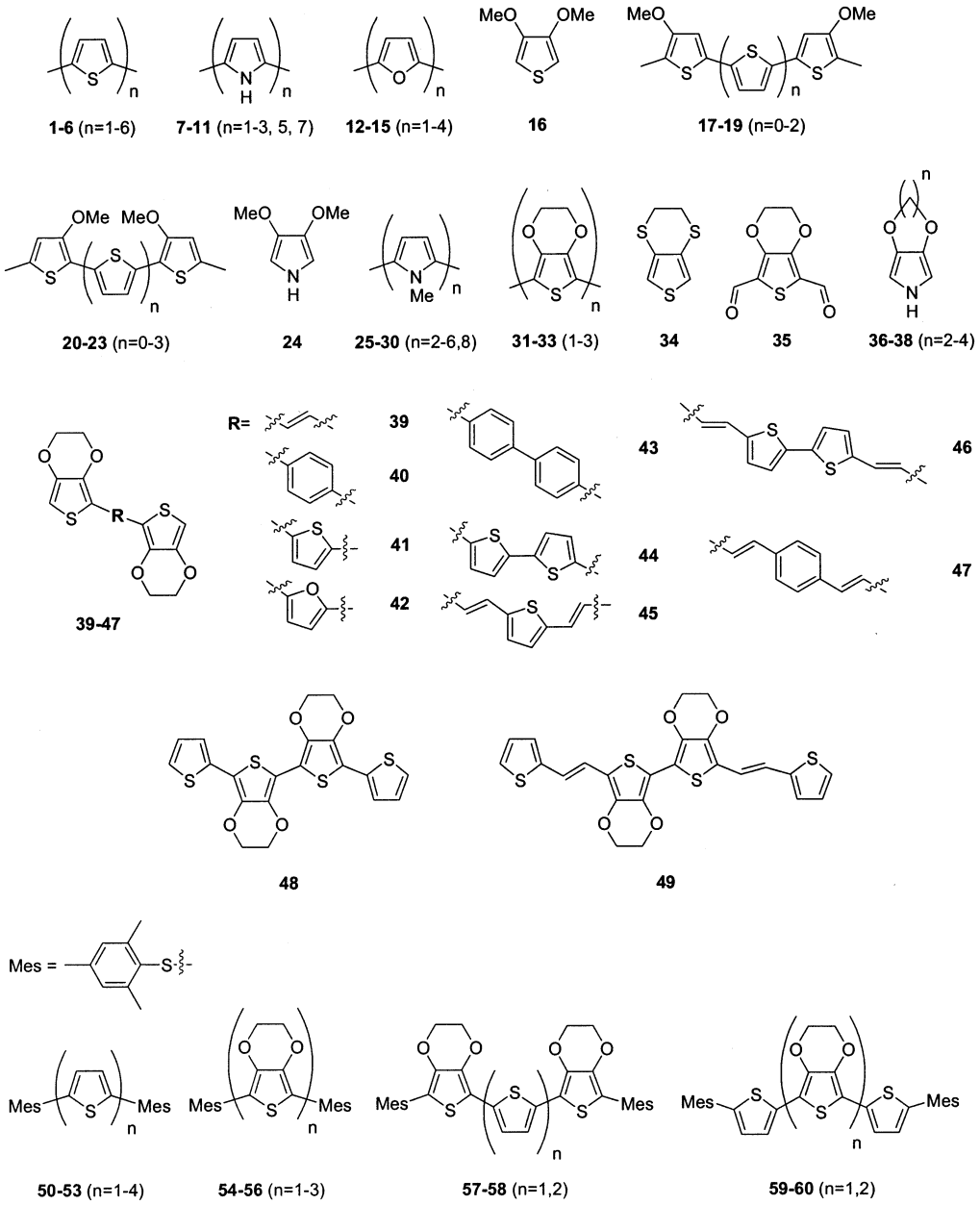

Figure 1. Molecular structures and labeling scheme used in the oligomer data set.

In the present contribution, we compare the performance of several widely used computational methodologies for predicting band gap energies applied to the above set of conjugated oligomers. We also consider what, if any, corrections may be applied to the computed excitation energies to improve accuracy as well as possible physical justification for these corrections. We also demonstrate that even for large oligomers having some 40−50 heavy atoms and 80 or more atoms overall, even relatively computationally demanding methods such as ab initio RPA or TDDFT can be performed using a reasonable basis set on normal desktop-level workstations without resorting to small or contracted basis sets, unrealistic approximations, or semiempirical methods.

II. Computational Methods

The 60 structures shown in Figure 1 were optimized using either the AM1 semiempirical method[50] with the GAMESS program[51] or by DFT with the B3LYP hybrid functional[52,53] in the 6-31G* basis set with the Q-Chem program.[54] These two procedures provide two sets of coordinates for evaluation of the excitation energies. Single-point calculations were performed with six different widely used methods for computing excitation energies without explicit solvent correction. The ZINDO semiempirical method was performed at the CIS level with the ZINDO program[36] and an active space from the 10 highest occupied orbitals and the 10 lowest unoccupied orbitals,[36] and also at the RPA level using the CEO program, which effectively employs a full active space.[55−57] Ab initio calculations were performed at both the CIS and RPA levels with the 6-31G* basis set using Q-Chem,[54] and time-dependent density functional theory was performed with the BLYP functional[53] in the 6-31G* basis set both with the Tamm-Dancoff approximation[58] and in full form. The BLYP functional was chosen for similarity with the B3LYP hybrid functional used to optimize the geometries and because it was shown to be one of the most accurate methods for aromatic hydrocarbons and polyenes.[59,60] Diffuse functions were not added to the basis set for HF and TDDFT calculations because for these extended structures, the predominant excited-state transition is a valence transition, and thus is not expected to have significant Rydberg-type character.

In all cases, the excitation with the largest calculated oscillator strength is taken as the excitation energy (Ω_{max}, analogous to the λ_{max} in experimental measurements). The excitation energy is used for theory-experiment comparisons instead of λ_{max} to allow equal treatment of error across a wide range of energies. For example, an error of 1 nm in wavelength corresponds to 0.031 eV at 200 nm but 0.006 eV at 460 nm. For all molecules having more than one conjugated ring, the excitation with the greatest calculated oscillator strength is found, in fact, to be the lowest excitation energy and is dominated by the HOMO−LUMO $\pi-\pi^*$ transition. This criterion indicates how accurate a particular computational method is when compared to experimental optical data, which considers excitation wavelength or energy and absorption intensity, since different methods may assign different transitions as having the greatest oscillator strengths. The effectiveness of a computational method will be determined, for our purposes, both by the accuracy of the resulting transition energies and by the accuracy of the predicted oscillator strengths. In all molecules consisting of greater than one monomer unit, the predicted oscillator strength of the principal transition is significantly larger than that of any other. However, in some single-ring molecules such as **1**, **7**, **12,** and **16**, two transitions are predicted to have very similar oscillator strengths but at different excitation energies, so that in these cases errors in the computed oscillator strength may lead to incorrect transition assignments.

To simplify reference to specific calculations in the following discussion, we adopt a notation referring to the single-point method performed on the predicted geometry from a specific geometry optimization. For example, ZINDO/CIS (AM1) refers to using the ZINDO semiempirical method at the CIS level on structures from AM1 geometry optimizations, while HF/RPA (DFT) refers to using ab initio RPA level excitation calculations on structures with DFT geometry optimization. In the case of the time-dependent DFT methods, TDDFT/CIS refers to the Tamm-Dancoff approximate TDDFT method[58] and TDDFT/RPA refers to full time-dependent DFT.[58,59,61]

III. Results

The experimental absorption energies,[5,7,9,37−48] given here as Ω_{max} in eV to facilitate comparison across a range of energies, as well as deviations of the computed values for each of the six single-point methods using both AM1 and DFT predicted geometries, are presented in Table 1. The solvents used in the experimental measurements and the literature references for each entry are given in Table 2. A summary of the statistical analysis of the data from each of the twelve methodologies can be found in Table 3.

As indicated by the average errors compiled in Table 3, all of the single-point computational methods show overall skew toward either systematically under-predicting or over-predicting optical absorption energies, with the exception of ZINDO/CIS, which is parametrized explicitly for predicting excitation energies in π-conjugated organic molecules.[36] To correct for these skews, linear regressions were performed on the data sets from each methodology, and these are plotted in Figures 3 and 4. If these regressions are used to correct empirically the computed excitation energies, by scaling by the regression slope and adding the regression intercept, all methods have significantly smaller errors—listed in Table 3 as the "corrected RMS errors".

A. ZINDO/CIS. Overall, for the present neutral organic molecules, the standard ZINDO/CIS method with an active space of 10 occupied and 10 unoccupied orbitals proves both to be the most accurate method for computing optical transitions before empirical corrections via linear regressions and to have the smallest systematic error (given by the average deviation in Table 3). For both AM1 and DFT predicted geometries, the overall errors are quite small (RMS errors of 0.37 eV and 0.31 eV, respectively). As might be expected for a method originally parametrized for organic π-system excitation energies,[36] the average error shows no skew toward either over-prediction or under-prediction, and the slope of the regressions indicated in Figures 2a and 3a are the closest to 1.0 for all the methods considered in this study.

The largest error for both sets of geometries arises from molecule **34**, which has two thioether functional groups (Figure 1). Similarly, structures which involve thiomesityl protecting groups (indicated by Mes- in Figure 1), especially molecules **50** and **54,** incur very large errors. This may indicate a weakness in modeling nonconjugated sulfur substituents for ZINDO/CIS, although there are insufficient samples of this sort in this data set for clear statistics. For some molecular structures, especially those having one heterocyclic ring, the DFT-predicted geometries give larger errors than those for AM1 but, in general, DFT geometries give more accurate predictions of band gaps.

B. ZINDO/RPA. As mentioned previously, the ZINDO semiempirical method was originally parametrized for a set of small molecules, by performing CIS computations on an active space of 10 occupied and 10 unoccupied orbitals.[36] Previous studies however, have also used the ZINDO model for RPA calculations,[55−57,62] which should, in principle, give more accurate oscillator strengths. Additionally, instead of using a fixed active space for the calculation, a Krylov-space algorithm can be used to effectively give a full treatment over all orbitals in a reasonable amount of computational time.[57]

Unfortunately, the present results indicate that the ZINDO/RPA approach performs less satisfactorily overall than ZINDO/CIS, showing a substantial skew toward under-predicting excitation energies, a large scatter as seen in Figures 2b and 3b, and a distinct separation between the monomer molecule data in the upper right portions of the graphs and the remainder of the data set. All three deficiencies are most likely symptomatic of a need for a different semiempirical RPA parametrization than for semiempirical CIS. Previous work showed that for a variety of organic aromatic molecules, the ZINDO/RPA approach provided a systematic under-prediction of excitation energies relative to ZINDO/CIS, and use of a full active space generally did not improve the computation.[62] Formally, the RPA calculation includes in the excitation manifold terms that correlate the excited stated beyond CIS.[63] This will lower the excitation energy compared to CIS, for any arbitrary choice of model Hamiltonian parameters. In principle, other semiempirical models could be used with the RPA method,[55] but since no semiempirical models have been parametrized for such RPA calculations as ZINDO was for CIS, other methods such as AM1 or PM3 are not likely to be substantially more reliable.

For both AM1- and DFT-predicted geometries, the overall errors are quite large (RMS errors of 0.89 eV and 0.81 eV, respectively) and while empirical correction via linear regression decreases the RMS errors, they are still the largest for the computational methods considered (corrected RMS errors of 0.44 eV and 0.37 eV for AM1 and DFT geometries, respectively). The largest absolute error in computed excitation energies for both AM1- and DFT-predicted geometries is for molecule **28**, a pentamer of *N*-methylpyrrole, although several monomeric molecules such as **34** also exhibit large errors and large scatter around the linear regression line.

TABLE 1: Comparison of Deviations from Experimental Absorption Energies as Computed by Various Methodologies[a]

		ZINDO/CIS		ZINDO/RPA		HF/CIS		HF/RPA		TDDFT/CIS		TDDFT/RPA	
molecule	expt	AM1	DFT	AM1	DFT	AM1	DFT	AM1	DFT	AM1	DFT	AM1	DFT
1	5.10	0.15	0.16	0.88	0.95	1.40	1.93	1.05	1.71	0.88	1.08	0.77	0.70
2	4.11	−0.17	−0.06	−1.13	−1.03	0.59	0.56	0.31	0.28	0.10	0.02	−0.20	−0.28
3	3.50	−0.26	−0.14	−1.04	−0.94	0.46	0.44	0.21	0.19	−0.15	−0.22	−0.41	−0.47
4	3.18	−0.33	−0.21	−1.00	−0.90	0.40	0.37	0.18	0.15	−0.35	−0.41	−0.55	−0.61
5	2.98	−0.37	−0.25	−0.97	−0.87	0.38	0.34	0.17	0.13	−0.51	−0.56	−0.65	−0.71
6	2.87	−0.41	−0.30	−0.97	−0.87	0.34	0.30	0.14	0.09	−0.65	−0.71	−0.76	−0.82
7	5.96	−0.28	−0.08	−0.14	−0.01	0.96	1.21	0.56	0.83	0.89	1.11	0.44	0.68
8	4.49	−0.27	−0.04	−1.24	−1.03	0.60	0.91	0.31	0.62	0.16	−0.01	−0.18	0.05
9	3.91	−0.34	−0.11	−1.14	−0.06	0.45	0.76	0.20	0.52	−0.23	−0.05	−0.47	−0.26
10	3.38	−0.33	−0.12	−1.00	−0.81	0.36	0.88	0.16	0.69	−0.64	−0.34	−0.76	−0.43
11	3.25	−0.42	−0.04	−0.58	−0.72	0.24	0.74	0.06	0.56	−0.95	−0.64	−1.01	−0.69
12	5.93	−0.53	−0.39	0.57	0.73	0.73	0.99	0.32	0.59	0.71	0.94	0.23	0.48
13	4.40	−0.33	−0.15	−0.81	−0.60	0.49	0.78	0.18	0.48	0.16	0.34	−0.23	−0.02
14	3.78	−0.42	−0.23	−0.71	−0.49	0.31	0.59	0.06	0.35	−0.20	−0.05	−0.50	−0.32
15	3.43	−0.25	−0.25	−0.63	−0.41	0.24	0.52	0.02	0.30	−0.44	−0.29	−0.66	−0.49
16	4.90	0.52	0.60	0.62	0.75	1.61	2.03	1.26	1.80	0.19	0.33	0.16	0.24
17	3.76	0.12	0.05	−0.87	−0.94	1.04	0.66	0.79	0.39	−0.10	−0.27	−0.26	−0.51
18	3.19	−0.06	0.06	−0.84	−0.74	0.65	0.63	0.41	0.39	−0.22	−0.31	−0.43	−0.51
19	2.96	−0.14	−0.07	−0.81	−0.04	0.60	0.57	0.39	0.35	−0.37	−0.48	−0.52	−0.62
20	3.81	0.43	−0.20	−0.66	−1.22	1.68	0.62	1.43	0.33	−0.04	−0.15	−0.09	−0.44
21	3.23	−0.08	−0.15	−0.89	−0.95	0.92	0.58	0.68	0.33	−0.11	−0.23	−0.27	−0.46
22	2.99	−0.20	−0.20	−0.89	−0.89	0.68	0.48	0.46	0.25	−0.30	−0.42	−0.44	−0.60
23	2.83	−0.14	−0.21	−0.77	−0.83	0.76	0.45	0.56	0.24	−0.37	−0.55	−0.47	−0.68
24	5.58	−0.22	−0.15	−0.35	−0.13	1.25	1.60	0.84	1.87	−0.45	0.13	−0.46	0.03
25	4.96	−0.50	−0.20	−1.50	−1.23	0.46	0.86	0.17	0.60	−0.33	−0.12	−0.57	−0.31
26	4.58	−0.69	−0.36	−1.54	−1.26	0.20	0.61	−0.04	0.38	−0.79	−0.56	−0.95	−0.69
27	4.44	−0.63	−0.21	−1.46	−1.12	0.28	0.79	0.06	0.58	−1.09	−0.76	−1.15	−0.81
28	4.35	−0.91	−0.60	−1.65	−1.39	−0.10	0.26	−0.30	0.07	−1.36	−1.13	−1.45	−0.71
29	4.34	−0.65	−0.49	−1.46	−1.31	0.22	0.37	0.01	0.18	−0.58	−1.25	−0.78	−1.28
30	4.32	−0.59	−0.25	−1.41	−1.13	0.29	0.71	0.09	0.51	−1.15	−0.77	−1.18	−0.80
31	4.82	0.50	0.47	0.66	0.73	1.63	1.91	1.28	1.66	0.27	0.29	0.13	0.07
32	3.87	−0.11	−0.05	−1.12	−1.08	0.90	0.78	0.62	0.49	0.23	0.11	−0.08	−0.23
33	3.10	0.08	0.02	−0.84	−0.79	0.95	0.81	0.70	0.56	0.17	0.05	−0.07	−0.20
34	4.38	0.95	1.06	1.09	1.26	1.55	2.02	1.25	1.81	−0.16	−0.15	−0.25	−0.22
35	3.83	0.38	0.33	−0.39	−0.45	1.41	1.22	1.10	0.90	0.38	0.34	0.13	0.05
36	5.58	0.16	0.27	−0.26	−0.15	1.29	1.48	0.89	1.77	−0.32	0.03	−0.32	0.54
37	5.93	−0.20	−0.04	−0.65	−0.52	0.93	1.17	0.52	0.78	−0.47	−0.35	−0.56	−0.44
38	5.90	−0.15	0.02	−0.67	−0.49	0.90	1.19	0.50	0.80	−0.43	0.21	−0.50	−0.34
39	3.45	0.06	0.05	−0.80	−0.80	0.87	0.73	0.62	0.48	0.09	0.09	−0.12	−0.24
40	3.60	0.10	0.30	−0.76	−0.60	0.72	0.90	0.47	0.65	−0.27	−0.26	−0.43	−0.40
41	3.32	−0.20	−0.11	−1.01	−0.92	0.67	0.61	0.42	0.36	−0.09	−0.17	−0.32	−0.41
42	3.43	−0.27	−0.11	−0.84	−0.69	0.57	0.74	0.32	0.50	−0.19	−0.19	−0.42	−0.39
43	3.63	0.22	0.35	−0.65	−0.55	0.76	0.86	0.53	0.62	−0.59	−0.60	−0.67	−0.67
44	3.01	−0.24	−0.14	0.54	−0.84	0.58	0.52	0.35	0.29	−0.26	−0.34	−0.44	−0.52
45	2.89	0.04	0.02	−0.62	−0.65	0.73	0.56	0.51	0.34	−0.14	−0.21	−0.35	−0.46
46	2.73	0.06	−0.05	−0.56	−0.66	0.81	0.51	0.61	0.30	−0.35	−0.43	−0.46	−0.60
47	3.15	0.26	0.24	−0.02	−0.04	0.74	0.65	0.53	0.43	−0.33	−0.40	−0.50	−0.58
48	2.98	−0.22	−0.16	−0.90	−0.85	0.65	0.54	0.43	0.31	−0.16	−0.24	−0.36	−0.46
49	2.69	0.00	−0.07	−0.62	−0.68	0.79	0.54	0.59	0.33	−0.24	−0.31	−0.40	−0.52
50	4.11	0.67	0.99	0.47	−0.37	0.76	1.15	0.52	0.90	−0.60	−0.05	−0.88	−0.15
51	3.46	0.35	0.39	−0.60	−0.59	0.91	0.75	0.68	0.51	−0.48	−0.21	−0.55	−0.55
52	3.21	−0.12	0.08	−0.89	−0.71	0.49	0.57	0.26	0.34	−0.43	−0.51	−0.57	−0.62
53	2.95	−0.13	0.00	−0.80	−0.69	0.56	0.53	0.35	0.31	−0.49	−0.52	−0.59	−0.64
54	4.07	0.74	0.87	0.51	−0.54	1.15	1.15	0.89	0.89	−0.20	−0.29	−0.62	−0.34
55	3.43	0.10	0.19	−0.88	−0.80	0.82	0.76	0.57	0.50	−0.44	−0.19	−0.51	−0.52
56	3.09	−0.13	−0.07	−0.92	−0.88	0.74	0.57	0.50	0.32	−0.27	−0.42	−0.41	−0.57
57	3.09	−0.06	0.03	−0.86	−0.78	0.71	0.62	0.47	0.38	0.14	−0.41	−0.09	−0.55
58	2.71	0.02	0.23	−0.67	−0.48	0.79	0.88	0.79	0.66	0.57	−0.30	−0.33	−0.40
59	3.05	−0.03	0.10	−0.80	−0.69	0.67	0.62	0.44	0.38	−0.28	−0.26	−0.42	−0.51
60	2.88	−0.18	−0.11	−0.84	−0.79	0.59	0.49	0.37	0.27	−0.42	−0.44	−0.55	−0.62

[a] The first row gives the computational excited-state method, while the second row gives the method for predicting the molecular geometry. All values are in eV.

C. Hartree−Fock/CIS. Hartree−Fock/CIS is a commonly used method for correcting the Hartree−Fock excited states by consideration of additional particle-hole configurations. The energies computed by HF/CIS are expected to show consistent over-prediction of excitation energies, which can be seen in the average errors in Table 3 of +0.74 eV and +0.80 eV for AM1- and DFT-predicted geometries, respectively.

While the overall errors are quite large (RMS errors of 0.83 eV and 0.91 eV for AM1 and DFT geometries, respectively), the empirical correction produces considerable improvement and the corrected RMS errors are among the lowest of all methods (0.30 eV and 0.24 eV for AM1 and DFT geometries, respectively). Unlike the ZINDO semiempirical methods, HF/CIS gives larger errors overall with DFT geometries than with AM1

TABLE 2: Experimental Absorption Energies (in eV), Solvent Used, and References

molecule	expt	solvent	ref	expt	solvent	ref	expt	solvent	ref	expt	solvent	ref
1	5.10	CH_2Cl_2	37									
2	4.11	CH_2Cl_2	37	4.07	toluene	47	4.09	CH_3CN	9	4.11	$CHCl_3$	5
3	3.50	CH_2Cl_2	37	3.50	toluene	47	3.53	CH_3CN	9	3.49	$CHCl_3$	5
4	3.18	CH_2Cl_2	37				3.16	CH_3CN	9	3.18	$CHCl_3$	5
5	2.98	$CHCl_3$	7				3.00	CH_3CN	9			
6	2.87	CH_2Cl_2	38	2.88	DMF	48				2.87	$CHCl_3$	5
7	5.96	CH_3CN	7									
8	4.49	CH_3CN	7									
9	3.91	CH_3CN	7	3.89	MeOH	70						
10	3.38	CH_3CN	7									
11	3.25	CH_3CN	7									
12	5.93	CH_3CN	9									
13	4.40	CH_3CN	9	4.41	EtOH	9	4.38	dioxane	9			
14	3.78	CH_3CN	9	3.77	EtOH	9	3.75	dioxane	9	3.71	benzene	9
15	3.43	CH_3CN	9	3.44	EtOH	9	3.41	dioxane	9	3.38	benzene	9
16	4.90	CH_3CN	39									
17	3.76	$CHCl_3$	40									
18	3.19	$CHCl_3$	40									
19	2.96	$CHCl_3$	40									
20	3.81	$CHCl_3$	40									
21	3.23	$CHCl_3$	40									
22	2.99	$CHCl_3$	40									
23	2.83	$CHCl_3$	40									
24	5.58	CH_3CN	39									
25	4.96	CH_3CN	7									
26	4.58	CH_3CN	7									
27	4.44	CH_3CN	7									
28	4.35	CH_3CN	7									
29	4.34	CH_3CN	7									
30	4.32	CH_3CN	7									
31	4.82	CH_3CN	3									
32	3.87	$CHCl_3$	41	3.89	CH_2Cl_2	44						
33	3.10	$CHCl_3$	42									
34	4.38	$CHCl_3$	43									
35	3.83	CH_2Cl_2	44									
36	5.58	CH_3CN	39	5.64	H_2O	45						
37	5.93	H_2O	45									
38	5.90	H_2O	45									
39	3.45	$CHCl_3$	42									
40	3.60	$CHCl_3$	42									
41	3.32	$CHCl_3$	42									
42	3.43	$CHCl_3$	42									
43	3.63	$CHCl_3$	42									
44	3.01	CH_2Cl_2	44,46									
45	2.89	CH_2Cl_2	44									
46	2.73	CH_2Cl_2	46									
47	3.15	CH_2Cl_2	44									
48	2.98	CH_2Cl_2	44,46									
49	2.69	CH_2Cl_2	46									
50	4.11	CH_2Cl_2	37									
51	3.46	CH_2Cl_2	37									
52	3.21	CH_2Cl_2	37									
53	2.95	CH_2Cl_2	37									
54	4.07	CH_2Cl_2	37									
55	3.43	CH_2Cl_2	37									
56	3.09	CH_2Cl_2	37									
57	3.09	CH_2Cl_2	37									
58	2.71	CH_2Cl_2	37									
59	3.05	CH_2Cl_2	37									
60	2.88	CH_2Cl_2	37									

geometries. As with the ZINDO/CIS and ZINDO/RPA methods, HF/CIS incurs the largest errors for monomeric structures or for those having high degrees of torsional freedom. The maximum absolute error in computed excitation energy for AM1 geometries is found for molecule **20**, which is strongly nonplanar, while the maximum absolute error for DFT geometries is found for molecule **16**, suggesting that monomers are treated less well by HF/CIS in the relatively small basis used here.

D. Hartree−Fock/RPA. Since the RPA method includes the same terms as CIS but also includes treatment of deexcitation operators, the method should correct for some of the consistent over-predictions of the HF/CIS method. Indeed, Table 3 shows that RPA gaps are smaller than CIS for all geometries and Hamiltonians (as discussed previously). In the present work, molecules having extended conjugation show small errors in the computed excitation energies with HF/RPA even before empirical correction via linear regression, as seen in Figures 2d and 3d. For AM1-predicted geometries, the method even gives slight under-predictions for molecules **26** and **28**, although these molecules would be expected to have significant inter-

TABLE 3: Summary of Statistics for the Computational Methodologies Examined, Including Root-Mean-Squared Error, Average Absolute Error, Maximum Absolute Error, Average Error as an Indication of Red-Shift or Blue-Shift Skew, and the Root-Mean-Squared Error after Correction via the Linear Regressions Indicated in Figures 2 and 3

method		RMS err. (eV)	avg. abs. err. (eV)	max. abs. err. (eV)	avg. err. (eV)	corrected rms err. (eV)
ZINDO/CIS	AM1	0.36	0.29	0.95	−0.09	0.33
	DFT	0.31	0.22	1.06	0.01	0.29
ZINDO/RPA	AM1	0.89	0.83	1.65	−0.65	0.44
	DFT	0.81	0.74	1.39	−0.59	0.37
HF/CIS	AM1	0.83	0.74	1.68	0.74	0.30
	DFT	0.91	0.81	2.03	0.81	0.24
HF/RPA	AM1	0.59	0.49	1.43	0.48	0.31
	DFT	0.73	0.58	1.87	0.58	0.26
TDDFT/CIS	AM1	0.49	0.40	1.36	−0.23	0.36
	DFT	0.47	0.38	1.25	−0.21	0.28
TDDFT/RPA	AM1	0.56	0.48	1.45	−0.42	0.31
	DFT	0.52	0.47	1.28	−0.37	0.23

ring dihedral angles which may not be treated well by the AM1 method.[64−67] For example, the predicted geometry of molecule **26** shows average dihedral angles of 39.1° and 45.2° for AM1 and DFT optimizations, respectively, and the geometry of molecule **28** shows average dihedral angles of 39.6° and 43.9° for AM1- and DFT-optimized geometries, respectively. On the other hand, the maximum absolute error in computed excitation energy for AM1 geometries (as for HF/CIS) is found for molecule **20**, which is also obviously expected to exhibit large dihedral angles. The largest deviation from the experimental absorption energies for DFT-predicted geometries occurs with molecule **24**, which indicates that small species are described less well by HF/RPA in the relatively small basis used here. As with HF/CIS, the HF/RPA method gives overall larger errors with DFT geometries than with AM1 geometries.

E. TDDFT/CIS. The Tamm-Dancoff approximation can be applied to TDDFT as well as in a traditional application to TDHF. In this sense, TDA-TDDFT is akin to Hartree−Fock CIS.[58] The Tamm-Dancoff approximation can improve the speed of computation considerably, especially for large molecules, while retaining good accuracy.[58,59] As seen in Table 3, the TDDFT/CIS method gives almost as accurate predictions of

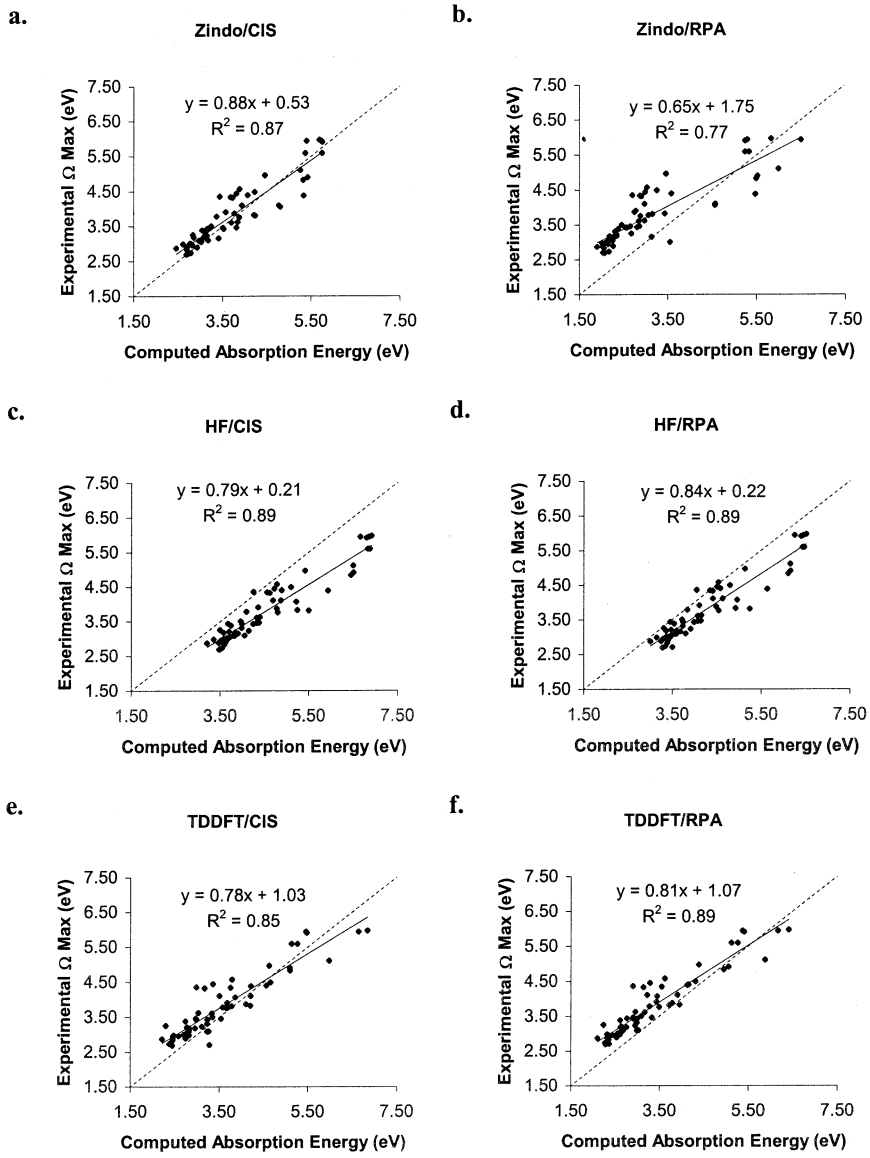

Figure 2. Comparisons between experimental Ω_{max} values and computed optical absorption energies for each single-point computational method using AM1-predicted molecular geometries. The solid lines are linear regressions with the formula and fit given. The dashed line indicates an ideal 1.0 correlation between experimental and calculated values.

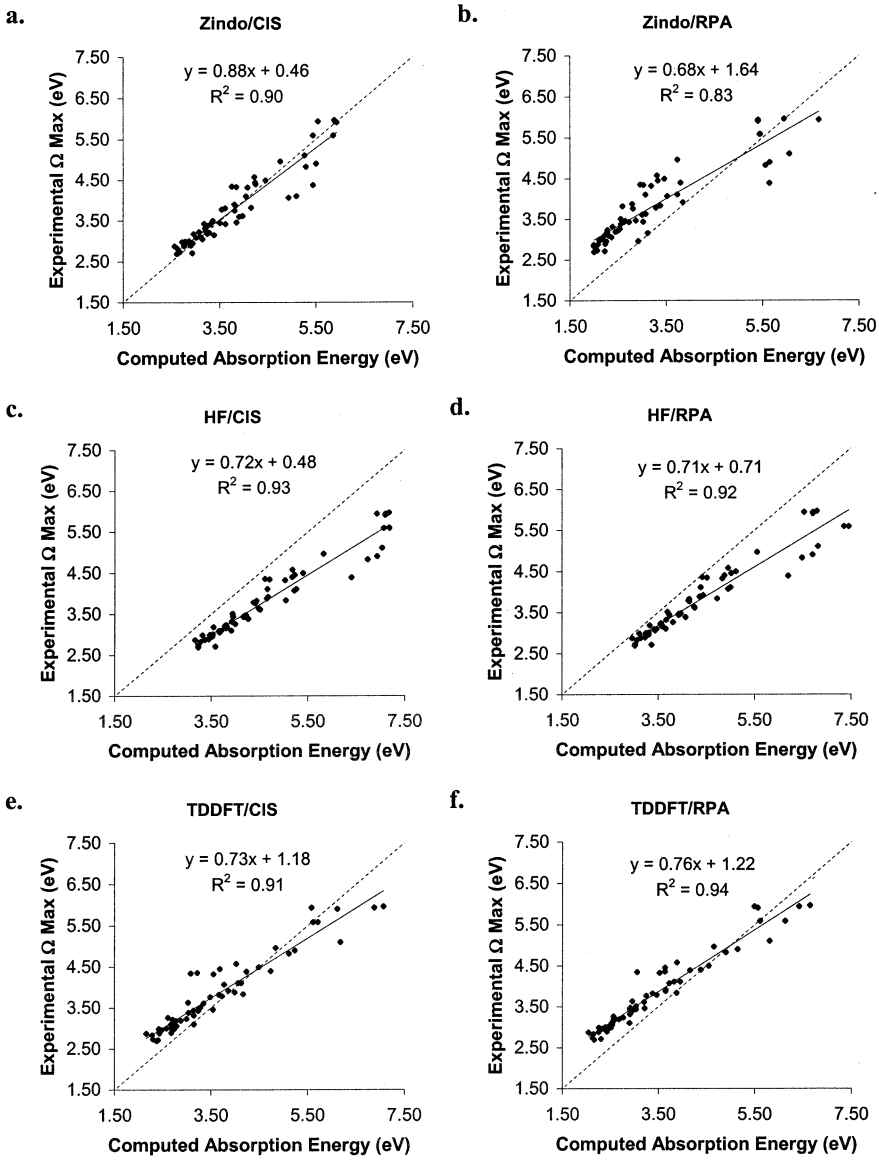

Figure 3. Comparisons between experimental Ω_{max} values and computed optical absorption energies for each single-point computational method using DFT-predicted molecular geometries. The solid lines are linear regressions with the formula and fit given. The dashed line indicates an ideal 1.0 correlation between experimental and calculated values.

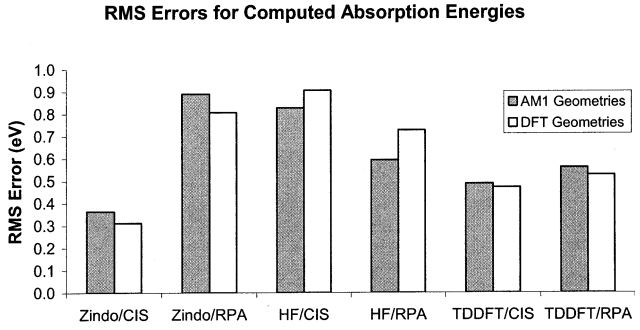

Figure 4. Overall comparison of RMS errors in computed band gaps for the 60-compound test set for all six single-point computational methods using both AM1- and DFT-predicted geometries. Notice that for all except the Hartree−Fock based methods, the DFT-computed geometries give the lesser overall errors.

band gap energies as ZINDO/CIS before the methods are corrected via linear regression, with RMS errors of 0.49 eV and 0.47 eV for AM1- and DFT-predicted geometries, respectively.

As with many of the other computational methods, molecules **28** and **29** yield the largest absolute errors for AM1- and DFT-predicted geometries, respectively. This may indicate that the TDDFT/CIS method has difficulty treating incomplete overlap in the π-system, although molecules such as **20**−**23** also have substantial torsions between monomer units, and these do not exhibit such large errors.

F. TDDFT/RPA. While the full TDDFT/RPA method yields significant under-prediction of excitation energies, especially for large molecules with small band gaps, as seen in the bottom left of Figures 2f and 3f, and in average errors of −0.42 eV and −0.38 eV for AM1 and DFT geometries, respectively, TDDFT/RPA has the smallest RMS errors after correction by linear regression. Thus, Figure 3f shows very little scatter around the line of best fit.

As with the TDDFT/CIS results, molecules **28** and **29** show the greatest deviations from experiment for AM1- and DFT-predicted geometries, respectively, although again molecules **20**−**23** do not show these problems and yet have substantial torsions.

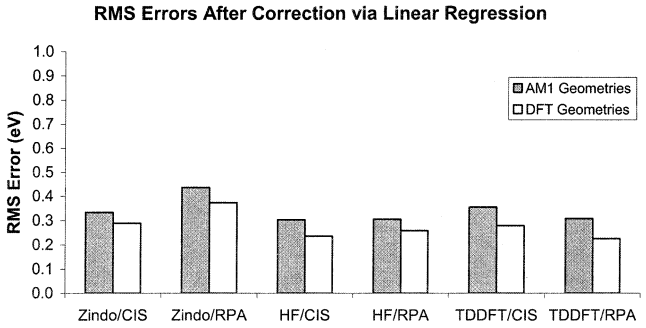

Figure 5. Comparison of RMS errors in computed absorption energies after correcting via linear regression for each method. Notice that most computational approaches give small errors that vary more with the particular geometry optimization method than with the single-point method.

IV. Discussion

As can be seen in Table 2, experimental band gap data for several compounds were reported in multiple solvents, which raises the question as to the need for computational solvent corrections. For molecules **14** and **15**, a trimer and tetramer of furan, the shift in optical absorption energies between samples measured in benzene and ethanol is reported to be 0.05 and 0.07 eV,[9] respectively—this is the largest solvatochromic shift found in the experimental measurements considered here, though the shift from benzene to ethanol represents a change of +23 in the static dielectric constant.[68] Molecule **14** has a computed excited-state dipole moment of 0.31 D compared to a 0.89 D ground-state dipole while molecule **15** has both negligible excited-state and ground-state dipole moments, both found using HF/CIS (DFT). The relatively small solvatochromism exhibited by these neutral molecules, even with such a large change in dielectric between polar and nonpolar solvents, is consistent with the small difference between ground-state and excited-state dipole moments in these largely symmetric oligomers and argues that solvent corrections are not in general necessary for these neutral species.

The basis set used for the HF/CIS, HF/RPA, TDDFT/CIS, and TDDFT/RPA calculations intentionally did not include diffuse functions. Figure 6 shows the effect of a larger basis set including diffuse functions, with the 6-31+G* basis set for a selection of the entire data set. The largest change in predicted absorption energy is found for the monomers and is likely due to the increased variational freedom as well as the increased Rydberg-like character in the transitions in these small π-systems. Figure 7 shows the difference in the trends of computed absorption energies between the two basis sets using the TDDFT/RPA (DFT) method, but the results for the other methods are quite similar. In particular, the slope and intercept of the linear regression change slightly due to the decreased error in the small molecules, but the effect is small since a substantial portion of the data set is largely unaffected by the addition of diffuse functions.

As mentioned previously, certain molecules incur large errors in calculated absorption energies by several methods. For example, oligomers of *N*-methylpyrrole (e.g., **28** and **29**) exhibit large errors with ZINDO/RPA and both TDDFT methods using both AM1 and DFT geometries. Similarly, molecule **20**, another molecule with large dihedral angles (average dihedral angles of 71.7° for the AM1-predicted geometry, although only 0.1° for the DFT-predicted geometry), has large errors using HF/CIS (AM1) and HF/RPA (AM1). However, TDDFT/CIS yields very small errors for this molecule (−0.04 eV and −0.09 eV for AM1- and DFT-predicted geometries, respectively).

Molecules with compact π-systems such as **1**, **7**, **12**, **16**, and **24** also show large errors in absorption energies for most of the computational methods considered here, although this is not unexpected since the methods predict vertical excitation energies from ground-state orbitals. The assumption that vertical processes dominate may not be so accurate in small molecules as for those with large, more expansive, easily polarized π-systems. The difference between the vertical excitation energies and the adiabatic excitations is likely to be small, but not entirely negligible and may partly explain the greater errors for small π-systems. Since the computational treatment yields strictly a vertical transition, there would be a slight overprediction in band gaps for small molecules and this should also show up in the line shapes of the experimental optical absorption spectra with the larger π-systems showing narrower 0→0 peak widths.

As discussed earlier, several monomers in the present study have more than one excitation with a large oscillator strength, and small errors in the predicted oscillator strength may potentially lead to incorrect transition assignments by the criterion used here. For example, molecule **1** is predicted to have two fairly strong absorptions by all computational methods. In particular, the DFT-predicted geometry shows excitations of 6.33 eV (0.117) and 7.03 eV (0.178) as predicted by HF/CIS,

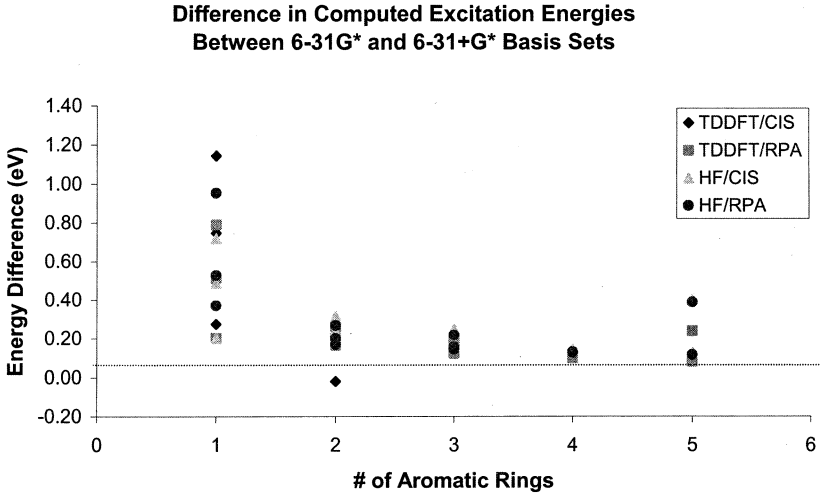

Figure 6. Comparison of absorption energies computed using DFT-predicted geometries for molecules **1**−**15** using either a 6-31G* basis set as used in the bulk of the work here, or the larger 6-31+G* basis set. Note that for the most part, the greatest disparities are observed with smaller, one-ring molecules such as **1**, **7**, and **12**.

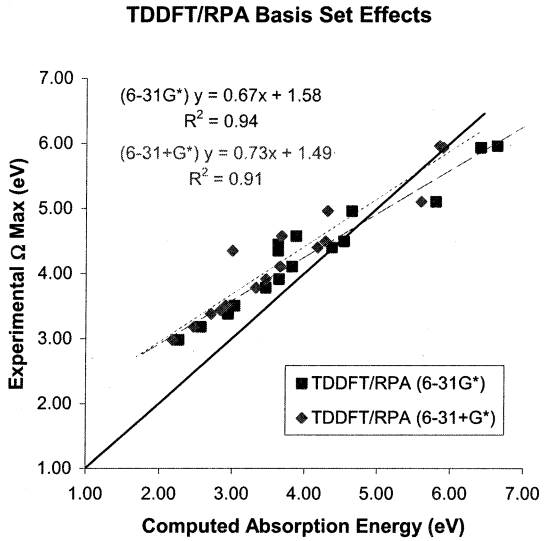

Figure 7. Comparison of computed absorption energies for molecules **1**−**5** with either the 6-31G* basis set used by the bulk of the work here, and the larger 6-31+G* basis set and the TDDFT/RPA (DFT) method. The slope and intercept of the linear fit changes slightly due to the smaller predicted absorption energies, but a significant *y*-intercept remains.

although the difference between the two excitations predicted by TDDFT/RPA is much smaller with excitations of 5.76 eV (0.064) and 5.81 eV (0.086). In the case of molecule **31**, two different states are chosen by TDDFT/CIS and TDDFT/RPA using the above assignment criterion. The two methods predict three relatively strong transitions at 4.99 eV (0.044), 5.12 eV (0.101), and 5.57 eV (0.063) by TDDFT/CIS and at 4.90 eV (0.105), 5.06 eV (0.023), and 5.29 eV (0.053) by TDDFT/RPA. Thus, the latter method assigns the strongest absorption to the lowest of the three transitions, while TDDFT/CIS assigns a higher-energy transition as the strongest.

For the present HF/CIS calculations, a simple one-parameter fit would be almost as effective as linear regression since the regression has a small intercept. The remaining methods appear to fit well to a single linear fit with the exception of ZINDO/RPA, but do exhibit significant intercepts. As shown in Figure 4, the smallest errors on average occur with the ZINDO/CIS method, in particular with DFT-predicted geometries. The uncorrected RMS error for this methodology is 0.31 eV, but after the empirical correction, the RMS error decreases to 0.29 eV. Figure 5 illustrates the substantially reduced RMS errors for all methods, upon correction with these linear regressions, which fall between 0.22 eV and 0.44 eV.

While a two-parameter fit will yield better results statistically, it is important to understand whether the parameters have physical meaning. A nonzero *y*-intercept implies finite experimental excitation energy despite a zero-energy computed value. Several effects may lead to this behavior, including greater solvatochromism for the larger and more polarizable molecules as well as (and probably more important) electronic localization due to torsional reduction of mixing, neither of which is explicitly treated in the present calculations. As mentioned earlier, the HF/CIS data do not exhibit a large *y*-intercept, although this effect may occur simply from cancellation of errors.

Of the potential effects which could lead to a finite *y*-intercept in the two-parameter linear regressions, several are doubtless due to the calculation methodologies used. For example, none of the HF or ZINDO methods treat electron correlation, although TDDFT/CIS and TDDFT/RPA methods do treat correlation and also exhibit finite intercepts. Although a finite basis was used and did not include diffuse functions, this was discussed above. While addition of diffuse functions changed the slope of the regressions, as indicated in Figure 7, the effect is not substantial as only the smallest molecules show pronounced changes in computed excitation energies. In short, while some of the slope and *y*-intercept may be due to these effects, there must be a physical basis for the effect, not simply a computational one.

Solvatochromism was discussed above and does not represent a very large effect for the present molecules and, moreover, is not expected to arise from the symmetric structure of most of the oligomers and the resulting small dipole moment differences. Further, if anything, solvatochromism generally stabilizes transitions in polar solvents such as CH_2Cl_2 which were used in the bulk of the experimental measurements compiled in Table 2. Thus, if solvation effects were important, the experimental absorption energies would be smaller than the computed absorption energies, rather than vice versa.

In short, the likely cause of the finite *y*-intercepts and small slopes for large molecules in the experimental versus computed band gap energy plots is vibrational and torsional localization. Although the oligomers in the present spectroscopic data set are not particularly long, they do likely experience torsional disorder and vibrational localization effects in solution.[69] While the computations are carried out at the equilibrium geometry, the experimental data do not necessarily arise from only this geometry. Localization effects would effectively decrease the conjugation length in the molecule and indeed result in greater experimental absorption energies than predicted.

Finally, while the results above compare single-point methods in detail, it is also useful to consider Figures 4 and 5, regarding the most reliable and accurate method for predicting geometries. While the AM1 semiempirical method is undoubtedly less computationally demanding than a full DFT geometry optimization with the 6-31G* basis as used here, it is clear that for all six single-point methods, especially after empirical correction via the linear regressions used here, the DFT geometries produce more consistent predictions of optical band gap energies.

V. Conclusions

Development of accurate, computationally practical methods for predicting optical band gaps for conjugated oligomers continues to present a challenge, but current electronic structure methods are becoming more satisfactory. Empirical corrections via linear regression can provide accurate predictions of molecule/oligomer absorption maxima with RMS errors as low as 0.23 eV. Even for neutral species, geometries predicted by the popular AM1 semiempirical method are not as consistently reliable for performing single-point excited-state calculations as are full DFT geometry optimizations. For both methods, remarkably, the semiempirical ZINDO/CIS method yields good agreement between experimental and computed optical absorption energies, with little need for additional correction for either solvent effects or systematic skew. On the other hand, TDDFT methods such as TDDFT/CIS and TDDFT/RPA become quite accurate after systematic empirical correction via linear regression.

Acknowledgment. We thank the NSF/MRSEC program for support through the Northwestern MRSEC (NSF DMR-96324732), ONR (N00014-02-1-0909) and the DoD MURI program for support. We are grateful to Dr. Sergei Tretiak and Prof. Shaul Mukamel for the CEO program for ZINDO/RPA calculations.

References and Notes

(1) Shirakawa, H.; Louis, E. J.; MacDiarmid, A. G.; Chiang, C. K.; Heeger, A. J. *J. Chem. Soc. Chem. Commun.* **1977**, 578−580.

(2) Heeger, A. J. *Angew. Chem., Int. Ed. Engl.* **2001**, *40*, 2591−2611.

(3) MacDiarmid, A. G. *Angew. Chem., Int. Ed. Engl.* **2001**, *40*, 2581−2590.

(4) Shirakawa, H. *Angew. Chem., Int. Ed. Engl.* **2001**, *40*, 2575−2580.

(5) Bäuerle, P. Sulfur-Containing Oligomers. In *Electronic Materials*: *The Oligomer Approach*; Müllen, K., Egner, G., Eds.; Wiley-VCH: Weinheim, 1998; pp 105−197.

(6) McCullough, R. D. *Adv. Mater.* **1998**, *10*, 93.

(7) Groenendaal, L.; Meijer, E. W.; Vekemans, J. A. J. M. Nitrogen-Containing Oligomers. In *Electronic Materials*: *The Oligomer Approach*; Müllen, K., Egner, G., Eds.; Wiley-VCH: Weinheim, 1998; pp 235−272.

(8) Glenis, S.; Benz, M.; LeGoff, E.; Schindler, J. L.; Kannewurf, C. R.; Kanatzidis, M. G. *J. Am. Chem. Soc.* **1993**, *115*, 12519−12525.

(9) Seixas de Melo, J.; Elisei, F.; Gartner, C.; Gaetano Aloisi, G.; Becker, R. S. *J. Phys. Chem. A* **2000**, *104*, 6907−6911.

(10) Kauffmann, T.; Lexy, H. *Chem. Ber.* **1981**, *114*, 3667−3673.

(11) Nalwa, H. S. *Handbook of Advanced Electronic and Photonic Materials and Devices*; Academic: San Diego, CA, 2000.

(12) Müllen, K.; Wegner, G. *Electronic Materials*: *The Oligomer Approach*; Wiley-VCH: Weinheim, New York, 1998.

(13) Brédas, J. L.; Cornil, J.; Beljonne, D.; dos Santos, D.; Shuai, Z. G. *Acc. Chem. Res.* **1999**, *32*, 267−276.

(14) Alper, J. *Science* **1989**, *246*, 208−210.

(15) Garnier, F. *Chem. Phys.* **1998**, *227*, 253−262.

(16) Würthner, F. *Angew. Chem., Int. Ed. Engl.* **2001**, *40*, 1037.

(17) Ho, P. K. H.; Kim, J.-S.; Burroughes, J. H.; Becker, H.; Li, S. F. Y.; Brown, T. M.; Cacialli, F.; Friend, R. H. *Nature* **2000**, *404*, 481−484.

(18) Pinner, D. J.; Friend, R. H.; Tessler, N. *Appl. Phys. Lett.* **2000**, *76*, 1137−1139.

(19) Inganäs, O.; Berggren, M.; Andersson, M. R.; Gustafsson, G.; Hjertberg, T.; Wennerström, O.; Dyreklev, P.; Granström, M. *Synth. Met.* **1995**, *71*, 2121−2124.

(20) Granström, M.; Petrisch, K.; Arias, A. C.; Lux, A.; Andersson, M. R.; Friend, R. H. *Nature* **1998**, *395*, 257.

(21) Ding, L.; Jonforsen, M.; Roman, L. S.; Andersson, M. R.; Inganäs, O. *Synth. Met.* **2000**, *110*, 113−140.

(22) Noda, T.; Ogawa, H.; Noma, N.; Shirota, Y. *J. Mater. Chem.* **1999**, *9*, 2177−2181.

(23) Grem, G.; Leising, G. *Synth. Met.* **1993**, *57*, 4105−4110.

(24) Berggren, M.; Inganäs, O.; Gustafsson, G.; Rasmusson, J.; Andersson, M. R.; Hjertberg, T.; Wennerström, O. *Nature* **1994**, *372*, 444−446.

(25) Campbell, I. H.; Smith, D. L. Electrical Transport in Organic Semiconductors. In *Topics in High Field Transport in Semiconductors*; Brennan, K. F., Ruden, P. P., Eds.; World Scientific: London, 2001; Vol. 22, pp 223−249.

(26) Mitschke, U.; Bäuerle, P. *J. Mater. Chem.* **2000**, *10*, 1471−1507.

(27) Kalinowski, J. *J. Phys. D*: *Appl. Phys.* **1999**, *32*, R179−R250.

(28) Grem, G.; Leditzky, G.; Ullrich, B.; Leising, G. *Adv. Mater.* **1992**, *4*, 36−7.

(29) Nelson, J. *Science* **2001**, *293*, 1059−1060.

(30) Di Marco, P.; Giro, G. *Appl. Phys.* (*N.Y.*) **1994**, *4*, 791−823.

(31) Roncali, J. *Chem. Rev.* **1997**, *97*, 173−205.

(32) Salzner, U.; Lagowski, J. B.; Pickup, P. G.; Poirier, R. A. *Synth. Met.* **1998**, *96*, 177−189.

(33) Salzner, U.; Pickup, P. G.; Poirier, R. A.; Lagowski, J. B. *J. Phys. Chem. A* **1998**, *102*, 2572−2578.

(34) Telesca, R.; Bolink, H.; Yunoki, S.; Hadziioannou, G.; Van Duijnen, P. T.; Snijders, J. G.; Jonkman, H. T.; Sawatzky, G. A. *Phys. Rev. B* **2001**, *6315*, 5112.

(35) Hutchison, G. R.; Zhao, Y.-J.; Freeman, A. J.; Ratner, M. A.; Marks, T. J. *submitted*.

(36) Ridley, J.; Zerner, M. *Theor. Chim. Acta* **1973**, *32*, 111−134.

(37) Hicks, R. G.; Nodwell, M. B. *J. Am. Chem. Soc.* **2000**, *122*, 6746−6753.

(38) Garcia, P.; Pernaut, J.-M.; Hapiot, P.; Wintgens, V.; Valat, P.; Garnie, F.; Delabouglise, D. *J. Phys. Chem.* **1993**, *97*, 513−516.

(39) Zotti, G.; Zecchin, S.; Schiavon, G.; Groenendaal, L. B. *Chem. Mater.* **2000**, *12*, 2996−3005.

(40) Miller, L. L.; Yu, Y. *J. Org. Chem.* **1995**, *60*, 6813−6819.

(41) Groenendaal, L.; Jonas, F.; Freitag, D.; Pielartzik, H.; Reynolds, J. R. *Adv. Mater.* **2000**, *12*, 481−494.

(42) Sotzing, G. A.; Reynolds, J. R.; Steel, P. J. *Chem. Mater.* **1996**, *8*, 882−889.

(43) Wang, C.; Schindler, J. L.; Kannewurf, C. R.; Kanatzidis, M. G. *Chem. Mater.* **1995**, *7*, 58−68.

(44) Mohanakrishnan, A. K.; Hucke, A.; Lyon, M. A.; Lakshmikantham, M. V.; Cava, M. P. *Tetrahedron* **1999**, *55*, 11745−11754.

(45) Schottland, P.; Zong, K.; Gaupp, C. L.; Thompson, B. C.; Thomas, C. A.; Giurgiu, I.; Hickman, R.; Abboud, K.; Reynolds, J. R. *Macromolecules* **2000**, *33*, 7051−7061.

(46) Turbiez, M.; Frère, P.; Blanchard, P.; Roncali, J. *Tetrahedron Lett.* **2000**, *41*, 5521−5525.

(47) Demanze, F.; Cornil, J.; Garnier, F.; Horowitz, G.; Valat, P.; Yassar, A.; Lazzaroni, R.; Brédas, J.-L. *J. Phys. Chem. B* **1997**, *101*, 4553−4558.

(48) Fichou, D.; Teulade-Fichou, M.-P.; Horowitz, G.; Demanze, F. *Adv. Mater.* **1997**, *9*, 75−80.

(49) Fichou, D.; Horowitz, G.; Xu, B.; Garnier, F. *Synth. Met.* **1990**, *39*, 243−59.

(50) Dewar, M. J. S.; Zoebisch, E. G.; Healy, E. F.; Stewart, J. J. P. *J. Am. Chem. Soc.* **1985**, *107*, 3902−3909.

(51) Schmidt, M. W.; Baldridge, K. K.; Boatz, J. A.; Elbert, S. T.; Gordon, M. S.; Jensen, J. H.; Koseki, S.; Matsunaga, N.; Nguyen, K. A.; Su, S. J.; Windus, T. L.; Dupuis, M.; Montgomery, J. A. *J. Comput. Chem.* **1993**, *14*, 1347−1363.

(52) Becke, A. D. *J. Chem. Phys* **1993**, *98*, 5648−5652.

(53) Lee, C.; Yang, W.; Parr, R. G. *Phys. Rev. B* **1988**, *37*, 785−789.

(54) Kong, J.; White, C. A.; Krylov, A. I.; Sherrill, C. D.; Adamson, R. D.; Furlani, T. R.; Lee, M. S.; Lee, A. M.; Gwaltney, S. R.; Adams, T. R.; Ochsenfeld, C.; Gilbert, A. T. B.; Kedziora, G. S.; Rassolov, V. A.; Maurice, D. R.; Nair, N.; Shao, Y.; Besley, N. A.; Maslen, P. E.; Dombroski, J. P.; Dachsel, H.; Zhang, W. M.; Korambath, P. P.; Baker, J.; Byrd, E. F. C.; Van Voorhis, T.; Oumi, M.; Hirata, S.; Hsu, C. P.; Ishikawa, N.; Florian, J.; Warshel, A.; Johnson, B. G.; Gill, P. M. W.; Head-Gordon, M.; Pople, J. A. *J. Comput. Chem.* **2000**, *21*, 1532−1548.

(55) Tretiak, S.; Saxena, A.; Martin, R. L.; Bishop, A. R. *Chem. Phys. Lett.* **2000**, *331*, 561−568.

(56) Mukamel, S.; Tretiak, S.; Wagersteiter, T.; Chernyak, V. *Science* **1997**, *277*, 781−787.

(57) Chernyak, V.; Schulz, M. F.; Mukamel, S.; Trtiak, S.; Tsiper, E. V. *J. Chem. Phys.* **2000**, *113*, 36−43.

(58) Hirata, S.; Head-Gordon, M. *Chem. Phys. Lett.* **1999**, *314*, 291−299.

(59) Hsu, C.-P.; Hirata, S.; Head-Gordon, M. *J. Phys. Chem. A* **2001**, *105*, 451−458.

(60) Hirata, S.; Lee, T. J.; Head-Gordon, M. *J. Chem. Phys.* **1999**, *111*, 8904−8912.

(61) Stratmann, R. E.; Scuseria, G. E.; Frisch, M. J. *J. Chem. Phys.* **1998**, *109*, 8218−8224.

(62) Baker, J. D.; Zerner, M. C. *J. Phys. Chem.* **1991**, *95*, 8614−8619.

(63) Linderberg, J.; Öhrn, Y. *Propagators in Quantum Chemistry*; Academic Press: London, New York, 1973.

(64) Quattrocchi, C.; Lazzaroni, R.; Bredas, J. L. *Chem. Phys. Lett.* **1993**, *208*, 120−4.

(65) Nino, A.; Munoz-Caro, C.; Senent, M. L. *THEOCHEM* **2000**, *530*, 291−300.

(66) Mohamed, A. A. *Int. J. Quantum Chem.* **2000**, *79*, 367−377.

(67) Carballeira, L.; Perez-Juste, I. *J. Comput. Chem.* **1998**, *19*, 961−976.

(68) *Handbook of Chemistry and Physics*; CRC Press: Boca Raton, FL, 1995.

(69) Yaliraki, S. N.; Silbey, R. J. *J. Chem. Phys.* **1996**, *104*, 1245−1253.

(70) Merrill, B. A.; LeGoff, E. *J. Org. Chem.* **1990**, *55*, 2904−2908.